Research Square

Preprints are preliminary reports that have not undergone peer review.
They should not be considered conclusive, used to inform clinical practice,
or referenced by the media as validated information.

Efficacy, Safety and Gut Microbiome Characteristics of Fecal Microbiota Transplantation and immunotherapy for Lung Cancer with Brain Metastases

Lanqun Qin
The Affiliated Changzhou No 2 People's Hospital of Nanjing Medical University
Dongqing Li
The Affiliated Changzhou No 2 People's Hospital of Nanjing Medical University
Chaoqun Wang
NMU: Nanjing Medical University
Danping Qian
The Affiliated Changzhou No 2 People's Hospital of Nanjing Medical University
Yanshuang Wei
The Affiliated Changzhou No 2 People's Hospital of Nanjing Medical University
Yufeng Qi
The Affiliated Changzhou No 2 People's Hospital of Nanjing Medical University
Li Tao
Nanjing Medical University
Pengyu Chen
NMU: Nanjing Medical University
Hua Jiang
The Affiliated Changzhou No 2 People's Hospital of Nanjing Medical University https://orcid.org/0000-0002-7871-4818
Qian Geng
karengq@njmu.edu.cn

The Affiliated Changzhou No 2 People's Hospital of Nanjing Medical University https://orcid.org/0000-0003-2351-5042

Research Article

Keywords: lung cancer, brain metastasis, gut-brain axis, fecal microbiota transplantation, immunotherapy

Posted Date: November 9th, 2026

DOI: https://doi.org/10.21203/rs.3.rs-11390617/v1

License: This work is licensed under a Creative Commons Attribution 4.0 International License.
Read Full License

Efficacy, Safety and Gut Microbiome Characteristics of Fecal Microbiota Transplantation and immunotherapy for Lung Cancer with Brain Metastases

Lanqun Qin[1,2*], Dongqing Li[1,2*], Chaoqun Wang[2], Danping Qian[1,2], Yanshuang Wei[2], Yufeng Qi[1,2], Li Tao[2], Pengyu Chen[2], Hua Jiang[1,2#], Qian Geng[1,2#]

[1] Oncology Department, The Third Affiliated Hospital of Nanjing Medical University, Changzhou Second People's Hospital, Changzhou, China; [2] Changzhou Medical Center, Nanjing Medical University, Changzhou, 213003, China;

*These authors contributed equally to this work

#Correspondences:

(Qian Geng is the main correspondence author and Hua Jiang is the secondary correspondence author)

Qian Geng, Oncology Department, The Third Affiliated Hospital of Nanjing Medical University, Changzhou Second People's Hospital, Changzhou, 213000, China, Email karengq@njmu.edu.cn.

Hua Jiang, Oncology Department, The Third Affiliated Hospital of Nanjing Medical University, Changzhou Second People's Hospital, Changzhou, 213000, China, Email czeyjh@njmu.edu.cn.

Abstract

Objective The blood-brain barrier (BBB) and central immunosuppressive microenvironment impair the efficacy of immunotherapy in lung-cancer patients with brain metastases (LCBM).

Fecal microbiota transplantation (FMT) remodels intestinal microecology to regulate central immunity via the gut-brain axis. This study aimed to explore the collaboration of FMT and immunotherapy in LCBM, and the potential mechanism by which FMT reshapes gut microbiota to improve intracranial therapeutic efficacy.

Methods Patients with LCBM who received FMT and immunotherapy at Changzhou Second People's Hospital between May 2024 and April 2026 were enrolled in this retrospective study. Intracranial and extracranial lesion responses were assessed according to RECIST version 1.1. Survival analysis was conducted using the Kaplan-Meier method, and safety was evaluated based on CTCAE version 5.0. Fecal metagenomic sequencing was performed for one representative patient with prominent clinical benefit to characterize shifts in gut-microbiota composition and function before and after FMT.

Results The final follow-up date was August, 2026, with a median follow-up of 10.5 months. The median age of enrolled 16 patients was 68 years (range 49-81 years); 68.75% (11/16) were male. Adenocarcinoma accounted for 93.75% (15/16). 56.25% (9/16) of patients had an ECOG-PS score ≥2. 75% (12/16) received one FMT session, and 50% (8/16) were treated in third-line or later settings. The intracranial objective response rate (ORR) was 37.5% and disease control rate (DCR) was 100%, with a median intracranial progression-free survival (iPFS) of 6.1 months. The extracranial ORR was 25.0% and DCR was 93.75%, with a median extracranial progression-free survival (ePFS) of 7.2 months. No significant efficacy difference was observed between patients with EGFR-TKI resistance and those without EGFR mutations. Most FMT-related adverse events were grade 1-2 self-limiting gastrointestinal reactions. Microbiota analysis of the beneficiary patient revealed severe baseline gut

dysbiosis characterized by over-enrichment of Firmicutes and near-depletion of Bacteroidetes. After FMT, microbial diversity was restored and elevated; the *Firmicutes/Bacteroidetes* ratio reached a balanced status. *Phocaeicola*, *Bacteroides* and butyrate-producing beneficial bacteria were markedly enriched while pathogenic bacteria were effectively suppressed, accompanied by substantial improvement in anti-tumor metabolic capacity of the gut microbiome.

Conclusion FMT is safe and feasible for patients with LCBM. By remodeling intestinal microecological balance, FMT achieves promising and durable intracranial disease control when combined with immonotherapy.

Keywords: lung cancer; brain metastasis; gut-brain axis; fecal microbiota transplantation; immunotherapy;

Introduction

Brain metastasis constitutes a major cause of mortality and functional impairment among patients with advanced lung cancer. Approximately 20%-40% of patients with advanced non-small-cell lung cancer (NSCLC) develop brain metastases, which generally indicate poor prognosis, deteriorated quality of life and increased clinical therapeutic difficulty[1]. Immune checkpoint inhibitors (ICIs) represented by PD-1/PD-L1 inhibitors have achieved remarkable progress in treating advanced NSCLC with negative driver-gene status or acquired driver-gene resistance. ICIs combined with platinum-based chemotherapy has become a widely adopted therapeutic regimen[2]. Nevertheless, the intracranial efficacy of

immunotherapy in LCBM remains less well characterized, partly because patients with active brain metastases have historically been underrepresented in or excluded from pivotal immune checkpoint inhibitor trials. Moreover, the blood–brain barrier (BBB), which restricts the passage of therapeutic agents and immune cells into the central nervous system (CNS), together with the intrinsically immunosuppressive CNS microenvironment, may limit the antitumor immune response within intracranial lesions[3,4]. Accordingly, improving immunotherapy responsiveness in patients with brain metastases remains an urgent unmet clinical need in lung-cancer management.

In recent years, the crosstalk between gut microbiota and host immunity, metabolism and the nervous system has attracted extensive attention. Although anatomically separated, the gut and brain communicate bidirectionally via neural pathways, immune mediators, microbial metabolites and neuroendocrine signals, the so-called gut-brain axis[5,6]. Under oncological conditions, BBB disruption facilitates the translocation of circulating immune cells and microbial metabolites into brain tissue, enabling gut microbiota to remotely modulate the intracranial immune microenvironment[7]. Previous studies have demonstrated reduced gut-microbiota diversity, community dysbiosis and depletion of short-chain-fatty-acid (SCFA)-producing bacteria in lung-cancer patients with brain metastases[8,9]. Gut microbes and their SCFA metabolites participate in tumor-associated inflammation and immune regulation. However, concrete clinical evidence linking gut microbiota to the immune microenvironment of brain metastatic lesions, as well as whether gut microbiota can directly influence immunotherapy efficacy, remains insufficient.

Fecal microbiota transplantation (FMT) transfers functional commensal bacteria isolated from healthy-donor stool into the recipient gastrointestinal tract to reconstruct and normalize gut microecology. Mounting evidence highlights the correlation between gut microbiome composition and ICIs efficacy[10,11]. Pre-clinical and clinical studies suggest that gut-microbiome profiles may predict immunotherapy responses, and FMT could potentially improve ICIs efficacy or reverse therapeutic resistance in selected populations[12-15]. For instance, FMT capsules derived from healthy donors combined with ICIs achieved a high objective response rate in patients with advanced melanoma, with adverse events dominated by low-grade gastrointestinal manifestations[16]. However, existing clinical evidence is largely derived from melanoma and other malignancies. The efficacy, safety and clinical value of FMT in lung cancer, particularly in patients with LCBM, have not been well characterized.

Given the above background, this retrospective study collected clinical data of LCBM receiving FMT and immuntherapy in our department from May 2024 to April 2026. We aimed to evaluate the potential clinical value and safety for this patient population and to conjecture the potential mechanism by which FMT reshapes gut microbiota to improve intracranial therapeutic efficacy in combination with immunotherapy.

Methods

Study Population

This retrospective study enrolled patients diagnosed with lung cancer and radiologically confirmed brain metastases who received FMT and immunotherapy in the Department of Oncology, Changzhou Second People's Hospital, from May 2024 to April 2026. The final follow-up cutoff date was August 27, 2026.

Inclusion criteria

1. Histologically or cytologically confirmed lung cancer;

2. Radiographically confirmed brain metastases with evaluable intracranial lesions;

3. Either driver-gene-negative disease, or acquired resistance to targeted therapy in patients with driver-gene-positive tumors;

4. Receipt of at least one cycle of FMT;

5. Prior receipt of immunotherapy or ongoing immunotherapy;

6. Availability of baseline and at least one post-FMT radiological assessment.

Baseline demographic data, ECOG-PS scores, PD-L1 expression profiles, driver-gene status, lines of prior therapy, treatment regimens and FMT administration cycles were collected. This study was approved by the Ethics Committee of Changzhou Second People's Hospital (Ethics No. [2025]YLJSA086).

FMT Administration

Oral FMT capsules were provided by Chenge Biotechnology Co., Ltd. (Xiamen, China). In addition to standard donor screening, comprehensive health assessment was performed for stool donors to guarantee biosafety. Each 10-capsule batch contained ≥2.5×10^{12} viable bacteria. Capsules were administered orally under fasting conditions. Each FMT course consisted of 30 capsules; 2-3 capsules were taken every 3-5 min until complete ingestion.

Efficacy Evaluation and Survival Follow-up

Baseline and post-treatment imaging datasets were re-reviewed by dedicated radiologists. Systemic tumor responses were evaluated per RECIST version 1.1, including complete

response (CR), partial response (PR), stable disease (SD) and progressive disease (PD). ORR was defined as the proportion of evaluable patients achieving CR and PR. DCR represented the proportion of evaluable patients achieving CR, PR and SD.

Intracranial progression-free survival (iPFS): time from FMT initiation until intracranial tumor enlargement, new brain-metastasis emergence, or death from any cause (whichever occurred first). Extracranial progression-free survival (ePFS): time from FMT initiation until extracranial disease progression or death from any cause. Overall survival (OS): time from FMT initiation until death from any cause. Patients alive without disease progression at the final follow-up were censored at the last follow-up time-point.

Safety assessments were performed according to CTCAE version 5.0. The occurrence, severity and spectrum of FMT-related adverse events were documented.

Statistical Analysis

Survival curves for PFS and OS were plotted with GraphPad Prism 8.0.1. Other statistical analyses were completed using SPSS 25.0. The Kaplan-Meier approach was applied for survival analysis, and the Log-Rank test was used for inter-group survival comparisons. A two-sided $p < 0.05$ was considered statistically significant.

Results

Baseline Patient Characteristics

Sixteen patients with LCBM receiving FMT were included. Thirteen patients (81.25%) received concurrent immunotherapy around FMT, three other patients had previously received immunotherapy. The median age was 68 years (range 49-81 years); 11 (68.75%)

patients were male. Fifteen patients (93.75%) had lung adenocarcinoma, and one patient had adenocarcinoma with neuroendocrine differentiation. Nine patients (56.25%) presented with ECOG-PS ≥ 2. Twelve patients (75%) received only one FMT infusion, and eight patients (50%) were treated in third-line or later settings. Seven patients had acquired EGFR-TKI resistance, and nine harbored no EGFR-driving mutations. Four (25%) received targeted therapy combined with immunotherapy and chemotherapy, six (37.5%) underwent chemotherapy combined with immunotherapy and another three (18.75%) received immunotherapy combined with targeted therapy. These three patients also received palliative cranial radiotherapy for brain metastases at the same time. Among them, one received stereotactic radiosurgery (SRS), while the other two cases underwent volumetric modulated arc therapy (VMAT). Baseline demographic and oncological features are summarized in **Table 1**.

Therapeutic Responses Following FMT

Imaging re-evaluation was performed for optimal intracranial and extracranial tumor responses and survival endpoints. No CR was observed for intracranial lesions. Six out of Sixteen patients (37.5%) achieved PR, and the remaining patients attained SD. The intracranial ORR was 37.5% and DCR was 100%. For extracranial lesions, four patients achieved PR and one patient developed PD manifested as pulmonary-lesion enlargement. Extracranial ORR was 25.0% and DCR was 93.75%. At the final follow-up on August 27 2026, the median follow-up duration was 10.5 months. The median iPFS and ePFS for the entire cohort were 6.1 months and 7.2 months, respectively **(Figure 1, Table 2)**.

In the EGFR-TKI-resistant subgroup (n = 7, median prior-therapy line = 3), one received SRS. Intracranial ORR was 42.9% (3/7) and DCR was 100% (7/7); extracranial ORR was 0% (0/7) and DCR was 85.7% (6/7). Median iPFS and ePFS were 6.8 months and 11.4 months. In the EGFR-wild-type subgroup (n = 9, median prior-therapy line = 2), two received WMAT. Intracranial ORR was 33.3% (3/9) and DCR was 100% (9/9); extracranial ORR was 44.4% (4/9) and DCR was 100% (9/9). Median iPFS and ePFS were 6.1 months and 7.2 months **(Figure 2)**.

Three patients (No. 8-10) received concurrent palliative cranial radiotherapy for large intracranial lesions (No.8/10 VMAT, No.9 SRS). The treatment regimen for these 3 patients were immunotherapy combined with targeted therapy. Patients No. 9 and No. 10 remained progression-free with PFS exceeding 12 months. Patient No. 8 obtained intracranial PR and extracranial SD despite relatively short PFS. Three patients (No. 5-7) received previous immunotherapy. Owing to the small sample size, it remains inconclusive whether prior immunotherapy or immunotherapy around FMT affects the therapeutic efficacy **(Table 2).**

Safety Profiles

Transient adaptive gastrointestinal manifestations occurred within 24-48 h after oral FMT-capsule administration, all graded 1-2: abdominal distension (31.25%), abdominal colic (18.75%), nausea and vomiting (25%). All symptoms were self-limiting and resolved spontaneously within 1-3 days without specific intervention. No grade ≥ 3 adverse events, severe infectious episodes or FMT-related deaths were observed **(Table 3)**.

Fecal Metagenomic Sequencing Before and After FMT

Fecal specimens from patient No. 12 were subjected to metagenomic sequencing to characterize FMT-driven gut-microbiome remodeling. This patient received first-line platinum-doublet chemotherapy plus immunotherapy followed by maintenance immunotherapy. He achieved durable disease control with ongoing progression-free survival over 22 months. Given no confounding effects from previous treatment, rendering this case highly representative. Two sampling time-points were selected: baseline (JSZH-C1) and after four FMT cycles with six cycles of systemic therapy (JSZH-RC1). The timeline for treatment, FMT interventions and sample collection is shown in **Figure 3A**.

Severe gut dysbiosis was detected at baseline: *Firmicutes (Bacillota)* dominated the gut community with a relative abundance of ~80%, whereas *Bacteroidetes (Bacteroidota),* a major phylum in healthy human stool, was nearly absent (~1%). This is consistent with the microbiota characteristics of LCBM reported in previous literature[17]. Substantial microbiome reconstruction was observed post-FMT **(Figure 3B)**. The relative abundance of *Firmicutes* decreased to ~52%, while Bacteroidetes increased sharply to ~43%, forming a dual-dominant phylum-level profile together with *Firmicutes*. The abundance of *Proteobacteria (Pseudomonadota)* dropped significantly. Although *Actinobacteria (Actinomycetota)* and Uroviricota showed statistically significant alterations, their relative abundances remained below 2%.

At the genus level, baseline microbiota were predominated by *Firmicutes* and *Enterobacteriaceae taxa* including *Blautia*, *Mediterraneanibacter*, *Escherichia*, *Enterocloster* and *Ruminococcus*. After FMT, the relative abundance of *Phocaeicola (Bacteroidetes)* rose from <1% to 22%, and *Bacteroides* increased from 1% to 12%. Concurrently, *Roseburia*,

Anaerostipes, *Parabacteroides*, *Dorea* and *Prevotella* were markedly enriched **(Supplementary Figure 1)**. Species-level alterations recapitulated genus-level findings. Baseline dominant species included *Mediterraneanibacter gnavus*, *Escherichia coli*, *Blautia wexlerae* and *Blautia sp. HCN-1074*. Post-FMT, four *Phocaeicola* species (*P. vulgatus*, *P. plebeius*, *P. coprocolla*, *P. dorei*), which were barely detectable at baseline, became prominent community members. Multiple butyrate-producing species including *Roseburia intestinalis*, *Anaerostipes hadrus*, *Anaerobutyricum hallii*, *Dorea longicatena* and *Flavonifractor plautii* bloomed. Meanwhile, opportunistic pathogens *Escherichia coli* and *Clostridioides difficile* were suppressed to extremely low levels **(Figure 4).** These observations indicated effective donor-strain engraftment and FMT-mediated gut-microbiota remodeling.

Functional metagenomic changes were concordant with taxonomic shifts. Thirty-eight significantly differentially abundant carbohydrate-active enzyme families were identified. Post-FMT enrichment of glycosyltransferases (GT2, GT4, GT41) and host-glycan-degrading hydrolases (GH29, GH92, GH20) matched the polysaccharide-utilization-locus (PUL) signature of *Phocaeicola*/*Bacteroides*. Baseline samples were enriched for Firmicutes-/Enterobacteriaceae-related enzymes such as GH1, GH3, GH32 and CE1 **(Supplementary Figure 2)**.

KEGG pathway analysis revealed that baseline microbiota featured high activity of membrane-transport modules (ABC transporters, phosphotransferase system), two-component systems and quorum-sensing pathways — functional hallmarks of facultative anaerobes such as *E. coli* under dysbiotic conditions. After FMT, pathways responsible for

ribosome biogenesis, aminoacyl-tRNA biosynthesis, purine/pyrimidine metabolism, peptidoglycan synthesis, amino-acid metabolism and secondary-metabolite biosynthesis were significantly up-regulated, suggesting restored completeness and diversity of microbial metabolic functions following donor-microbe engraftment **(Supplementary Figures 3-4)**.

Discussion

Compared with extracranial primary lesions, brain metastases possess unique immunosuppressive features. The blood-brain barrier and blood-cerebrospinal-fluid barrier restrict peripheral immune-cell infiltration, while microglia and astrocytes establish an immune-tolerant microenvironment[9]. In paired-sample immune profiling of NSCLC primary tumors and brain metastases reported by Kudo et al., brain-metastatic lesions exhibited impaired dendritic-cell maturation, repressed Th1 signaling and leukocyte-extravasation pathways, decreased T-cell infiltration, increased macrophage infiltration, and down-regulated vascular-cell-adhesion-molecule 1 (VCAM-1)[18]. This “immune-cold” phenotype explains the clinical scenario in which extracranial tumors respond to ICIs while intracranial lesions progress. Therefore, reshaping systemic immunity via peripheral interventions to facilitate effector-T-cell trafficking across the blood-brain barrier constitutes a core strategy for improving ICIs efficacy against brain metastases.

Most patients enrolled in our study were heavily pretreated LCBM; over half had ECOG-PS ≥ 2, and the cohort included refractory cases with EGFR-TKI resistance, closely mirroring real-world clinical populations. Even under these unfavorable baseline conditions, the median iPFS reached 6.1 months, exceeding historical outcomes of conventional palliative late-line therapy. In comparison, the CAP-Brain study investigated first-line Camrelizumab

plus Pemetrexed-Carboplatin for untreated non-squamous NSCLC with brain metastases and reported a median iPFS of 8.4 months[19]. Our result was only 2 months shorter, implying meaningful intracranial tumor-control potential of FMT when combined with immunotherapy. Notably, intracranial tumor shrinkage was observed in patient No.7 without concurrent immunotherapy, providing a potential alternative for patients with immunotherapy resistance or poor tolerance to ICIs.

Subgroup analyses demonstrated higher intracranial response rates in the EGFR-TKI-resistant subgroup, whereas the EGFR-wild-type subgroup achieved concurrent intracranial and extracranial disease control. The poor extracranial efficacy in patients with EGFR resistance might be related to the relatively later treatment lines. Prior investigations have proven that prolonged EGFR-TKI exposure alters gut microecology, reduces microbial diversity and enriches opportunistic pathogens, contributing to targeted-therapy resistance and systemic immunosuppression[20]. In our cohort, the EGFR-TKI-resistant subgroup obtained limited extracranial objective responses yet favorable intracranial tumor control. We hypothesize that FMT preferentially ameliorates the central immune microenvironment through the gut-brain axis; reversal of systemic tumor resistance may demand prolonged intervention or combination with additional systemic anti-tumor agents.

Safety is critical for novel interventional modalities in advanced malignancies. All FMT-related adverse events in this study were grade 1-2 self-limiting gastrointestinal manifestations. No grade ≥ 3 adverse events, severe infections or treatment-related deaths occurred. These findings are consistent with phase-II data of FMT combined with immunotherapy for advanced solid tumors published in *Nature Medicine*[15], where mild self-resolving gastrointestinal

symptoms predominated, and serious adverse events were largely attributable to immunotherapy rather than FMT manipulation. Our work further supports acceptable tolerability of oral FMT capsules even for advanced-stage patients with brain metastases and poor physical performance status.

Cranial radiotherapy represents an essential local therapeutic modality for brain metastases. The CTONG2003 trial first demonstrated that camrelizumab combined with chemotherapy and radiotherapy yielded a median iPFS of 12.7 months versus 9.9 months in the placebo arm for previously untreated NSCLC with brain metastases[21]. Another multi-center phase-II trial (C-Brain study) evaluated cranial radiotherapy plus camrelizumab and platinum-doublet chemotherapy, reporting an intracranial ORR of 78.5% and systemic ORR of 69.2%, superior to historical controls[22]. This highlights the potent anti-tumor activity of "radiotherapy-immunotherapy-chemotherapy" triple-modality therapy, especially for symptomatic patients with large intracranial lesions. Nevertheless, long-term sequelae including cognitive decline and radiation-induced brain injury cannot be overlooked[23]. In our study, two out of three patients receiving concurrent palliative cranial radiotherapy maintained progression-free status for >12 months. Concurrent FMT plus cranial radiotherapy may help reverse the "immune-cold" phenotype and enhance ICIs penetration across the blood-brain barrier. Radiotherapy triggers immunogenic tumor-cell death, and gut microbiota orchestrates systemic antigen presentation and T-cell activation to amplify the abscopal effect. This phenomenon has been validated in pre-clinical solid-tumor models, yet large-scale clinical evidence in lung-cancer patients with brain metastases remains absent and warrants further exploration[24].

Metagenomic analysis of the index case revealed microbiome alterations concordant with anti-tumor effects following FMT. First, donor-derived *Phocaeicola vulgatus*, *P. plebeius*, *P. coprocolla* and *P. dorei* became dominant taxa, accompanied by enrichment of PUL-associated glycoside-hydrolase and glycosyltransferase gene families (GT2, GH29, GH92, GH20), indicating successful reconstruction of donor-strain-encoded carbohydrate-metabolic capacity in the recipient gut. Second, multiple *Enterocloster* species and *Clostridium innocuum*, abundant at baseline, declined sharply post-FMT, consistent with observations from the FMT-LUMINate phase-II trial, in which responders exhibited clearance of *E. citroniae*, *E. lavallensis* and *C. innocuum*[15]. Pre-clinical animal experiments demonstrated that re-introducing these taxa abrogated ICIs-mediated anti-tumor efficacy. Third, simultaneous reduction of *E. coli*, Proteobacteria and *Clostridioides difficile* reflected alleviated intestinal inflammatory burden and suppressed overgrowth of facultative anaerobes, which may mitigate translocation of gut-derived pro-inflammatory mediators into the CNS and preserve blood-brain-barrier integrity.

Furthermore, restored SCFA-producing bacteria post-FMT are potentially linked to intracranial immune activation. The taxa blooming after FMT, namely *Roseburia intestinalis*, *Anaerostipes hadrus*, *Anaerobutyricum hallii* and *Dorea longicatena*, are well-established butyrate-/propionate-producers. Beyond maintaining intestinal-barrier homeostasis, butyrate and other SCFAs reach the brain via systemic circulation and modulate myeloid-cell function. Zhou et al. demonstrated that SCFAs promote M1-polarization of tumor-associated macrophages by reprogramming glycolytic metabolism, thereby suppressing intracranial tumor growth[25]. Erny et al. reported that SCFAs are indispensable for microglial maturation.

Therefore, restoration of SCFA-producing commensals in our case may constitute a metabolic foundation whereby FMT augments ICIs responses against brain metastases[26]. This hypothesis aligns with previous reports linking *Akkermansia muciniphila* to improved ICIs efficacy and the NADIM-II trial demonstrating that *Faecalibacterium prausnitzii* correlates with favorable PFS and OS in NSCLC patients receiving neoadjuvant chemo-immunotherapy[27,28].

This study has several limitations. First, as a small-sample retrospective investigation, confounding factors stemming from radiotherapy, chemotherapy and targeted therapy cannot be completely excluded, limiting the level of clinical evidence. Second, metagenomic sequencing was only performed for one representative patient and may not generalize to the whole cohort. Peripheral-blood and cerebrospinal-fluid cytokine and SCFA-metabolite measurements were lacking; hence, causal chains connecting "FMT-gut-microbiome-metabolites-intracranial immune microenvironment-tumor control" cannot be established, and only correlative relationships can be inferred. Third, this study did not address optimal FMT frequency, standardized donor-screening criteria, differential benefits across combination regimens, or predictive biomarkers for FMT responsiveness. Long-term engraftment stability of donor-derived microbiota and long-term safety profiles also require extended follow-up.

Conclusions

This is one of the few retrospective studies investigating FMT and immunotherapy for LCBM. From the perspectives of clinical efficacy, safety and gut-microecological remodeling, our data support the clinical feasibility of FMT and immunotherapy in LCBM and provide real-world evidence for gut-brain-axis-oriented therapeutic interventions for brain malignancy.

Ethics approval and informed consent

This study was approved by the Ethics Committee of Changzhou Second People's Hospital (Ethics No. [2025]YLJSA086). As this was a retrospective analysis of anonymized, routinely collected clinical data with no intervention or direct patient contact, the requirement for individual informed consent was waived by the Ethics Committee in accordance with national regulations.

Authors' contributions and Consent for publication

All authors made a significant contribution to the work reported, whether that is in the conception, study design, execution, acquisition of data, analysis and interpretation, or in all these areas; took part in drafting, revising or critically reviewing the article; gave final approval of the version to be published; have agreed on the journal to which the article has been submitted; and agree to be accountable for all aspects of the work.

Competing interests

The authors report no conflicts of interest in this work.

Data availability

The datasets used and/or analysed during the current study are available from the main correspondence author (Qian Geng) on reasonable request.

Funding

This study was supported by Annual Research Project of Menghe Medical School in Changzhou City (No. 20260198) and the Changzhou Science and Technology Plan Project (No. CJ20258010).

Acknowledgements

The authors would like to express their sincere gratitude to all patients and their families for their contributions to this study. We also thank the clinical staff of the Department of Oncology at Changzhou Second People's Hospital for their assistance with patient care, clinical data collection, and follow-up. We are grateful to all personnel who provided support for fecal sample collection and metagenomic sequencing analysis.

References

1. Gillespie CS, Mustafa MA, Richardson GE, et al. Genomic Alterations and the Incidence of Brain Metastases in Advanced and Metastatic NSCLC: A Systematic Review and Meta-Analysis. *J Thorac Oncol*. Dec 2023;18(12):1703–1713. doi:10.1016/j.jtho.2023.06.017

2. Hendriks LE, Kerr KM, Menis J, et al. Non-oncogene-addicted metastatic non-small-cell lung cancer: ESMO Clinical Practice Guideline for diagnosis, treatment and follow-up. *Ann Oncol*. Apr 2023;34(4):358–376. doi:10.1016/j.annonc.2022.12.013

3. Fares J, Ulasov I, Timashev P, Lesniak MS. Emerging principles of brain immunology and immune

checkpoint blockade in brain metastases. *Brain*. May 7 2021;144(4):1046–1066. doi:10.1093/brain/awab012

4. Hendriks LEL, Remon J, Menis J, Besse B. Is there any opportunity for immune checkpoint inhibitor therapy in non-small cell lung cancer patients with brain metastases? *Transl Lung Cancer Res*. Jun 2021;10(6):2868–2875. doi:10.21037/tlcr-20-343

5. Xu W, Xu Q, Luo P, et al. Gut-Brain-Microbiome Axis in the Regulation of Cancer Immune Escape and Immunotherapy in Tumors. *Research (Wash D C)*. 2025;8:0885. doi:10.34133/research.0885

6. Morad G, Damania AV, Melendez B, et al. Microbial signals in primary and metastatic brain tumors. *Nat Med*. Nov 2025;31(11):3675–3688. doi:10.1038/s41591-025-03957-4

7. Ahmed H, Leyrolle Q, Koistinen V, et al. Microbiota-derived metabolites as drivers of gut-brain communication. *Gut Microbes*. Jan–Dec 2022;14(1):2102878. doi:10.1080/19490976.2022.2102878

8. Shi M, Wang LF, Hu WT, Liang ZG. The gut microbiome in lung cancer: from pathogenesis to precision therapy. *Front Microbiol*. 2025;16:1606684. doi:10.3389/fmicb.2025.1606684

9. Jiang H, Zeng W, Zhang X, et al. Gut microbiota and its metabolites in non-small cell lung cancer and brain metastasis: from alteration to potential microbial markers and drug targets. *Front Cell Infect Microbiol*. 2023;13:1211855. doi:10.3389/fcimb.2023.1211855

10. Vetizou M, Pitt JM, Daillere R, et al. Anticancer immunotherapy by CTLA-4 blockade relies on the gut microbiota. *Science*. Nov 27 2015;350(6264):1079–84. doi:10.1126/science.aad1329

11. Routy B, Le Chatelier E, Derosa L, et al. Gut microbiome influences efficacy of PD-1-based immunotherapy against epithelial tumors. *Science*. Jan 5 2018;359(6371):91–97. doi:10.1126/science.aan3706

12. Du Y, Li Y, Yu M, et al. Fecal microbiota transplantation plus immune checkpoint inhibitor

411 rechallenges in patients with advanced non-small cell lung cancer: a single-arm exploratory study. *Transl*
412 *Lung Cancer Res*. Oct 31 2025;14(10):4541–4559. doi:10.21037/tlcr-2025-973
413 13. Davar D, Dzutsev AK, McCulloch JA, et al. Fecal microbiota transplant overcomes resistance to anti-
414 PD-1 therapy in melanoma patients. *Science*. Feb 5 2021;371(6529):595–602.
415 doi:10.1126/science.abf3363
416 14. Fernandes R, Jabbarizadeh B, Rajeh A, et al. Fecal microbiota transplantation plus immunotherapy
417 in metastatic renal cell carcinoma: the phase 1 PERFORM trial. *Nat Med*. Apr 2026;32(4):1325–1336.
418 doi:10.1038/s41591-025-04183-8
419 15. Duttagupta S, Messaoudene M, Hunter S, et al. Fecal microbiota transplantation plus
420 immunotherapy in non-small cell lung cancer and melanoma: the phase 2 FMT-LUMINate trial. *Nat Med*.
421 Apr 2026;32(4):1337–1350. doi:10.1038/s41591-025-04186-5
422 16. Routy B, Lenehan JG, Miller WH, Jr., et al. Fecal microbiota transplantation plus anti-PD-1
423 immunotherapy in advanced melanoma: a phase I trial. *Nat Med*. Aug 2023;29(8):2121–2132.
424 doi:10.1038/s41591-023-02453-x
425 17. Han X, Sun QG, Zang D, Chen J. Comprehensive fecal metagenomic and metabolomic analysis
426 reveals the role of gut microbiota and metabolites in detecting brain metastasis of small cell lung cancer.
427 *Front Microbiol*. 2025;16:1673983. doi:10.3389/fmicb.2025.1673983
428 18. Kudo Y, Haymaker C, Zhang J, et al. Suppressed immune microenvironment and repertoire in brain
429 metastases from patients with resected non-small-cell lung cancer. *Ann Oncol*. Sep 1 2019;30(9):1521–
430 1530. doi:10.1093/annonc/mdz207
431 19. Hou X, Zhou C, Wu G, et al. First-line camrelizumab plus pemetrexed and carboplatin for advanced
432 non-squamous non-small-cell lung cancer with brain metastases (CAP-BRAIN): final results of a

multicentre, open-label, single-arm, phase 2 trial in China. *EClinicalMedicine*. Dec 2025;90:103638. doi:10.1016/j.eclinm.2025.103638

20. Jiang T, Zhang M, Hao S, Huang S, Zheng X, Sun Z. Revealing the role of the gut microbiota in enhancing targeted therapy efficacy for lung adenocarcinoma. *Exp Hematol Oncol*. Feb 9 2024;13(1):15. doi:10.1186/s40164-024-00478-7

21. Li YS, Yu Q, Bu Q, et al. First-Line Camrelizumab Versus Placebo Plus Chemotherapy With or Without Radiotherapy for Brain Metastases in NSCLC: The CTONG 2003 Randomized Placebo-Controlled Trial. *J Thorac Oncol*. Jul 2025;20(7):928–940. doi:10.1016/j.jtho.2025.02.004

22. Xu Y, Chen K, Xu Y, et al. Brain radiotherapy combined with camrelizumab and platinum-doublet chemotherapy for previously untreated advanced non-small-cell lung cancer with brain metastases (C-Brain): a multicentre, single-arm, phase 2 trial. *Lancet Oncol*. Jan 2025;26(1):74–84. doi:10.1016/S1470-2045(24)00643-0

23. Gondi V, Deshmukh S, Brown PD, et al. Sustained Preservation of Cognition and Prevention of Patient-Reported Symptoms With Hippocampal Avoidance During Whole-Brain Radiation Therapy for Brain Metastases: Final Results of NRG Oncology CC001. *Int J Radiat Oncol Biol Phys*. Nov 1 2023;117(3):571–580. doi:10.1016/j.ijrobp.2023.04.030

24. Zhao LY, Mei JX, Yu G, et al. Role of the gut microbiota in anticancer therapy: from molecular mechanisms to clinical applications. *Signal Transduct Target Ther*. May 13 2023;8(1):201. doi:10.1038/s41392-023-01406-7

25. Zhou M, Wu J, Shao Y, et al. Short-chain fatty acids reverses gut microbiota dysbiosis-promoted progression of glioblastoma by up-regulating M1 polarization in the tumor microenvironment. *Int Immunopharmacol*. Nov 15 2024;141:112881. doi:10.1016/j.intimp.2024.112881

455 26. Erny D, Hrabe de Angelis AL, Jaitin D, et al. Host microbiota constantly control maturation and
456 function of microglia in the CNS. *Nat Neurosci*. Jul 2015;18(7):965–77. doi:10.1038/nn.4030
457 27. Derosa L, Routy B, Thomas AM, et al. Intestinal Akkermansia muciniphila predicts clinical response
458 to PD-1 blockade in patients with advanced non-small-cell lung cancer. *Nat Med*. Feb 2022;28(2):315–
459 324. doi:10.1038/s41591-021-01655-5
460 28. Serna-Blasco R, Festa AR, Sanz-Moreno S, et al. Abstract 6684: Impact of fecal microbiome on the
461 efficacy of neoadjuvant chemo-immunotherapy and colitis adverse events: Findings from the NADIM II
462 Trial. *Cancer Research*. 2024;84(6_Supplement):6684 – 6684. doi:10.1158/1538-7445.Am2024-6684
463

464 **Table 1** Patient and Tumor Characteristics.

465

Characteristics	No. of Patients (%)
Age (Median ± SD, years)	68 ± 9.5
Oncology type Adenocarcinoma Adenocarcinoma with neuroendocrine differentiation	 15 (93.75) 1 (6.25)
Gender Men Women	 11 (68.75) 5 (31.25)
Treatment line 1 2	 4 (25.00) 4 (25.00)

≥3	8 (50.00)
Performance status score	
0-1	7 (43.75)
≥2	9 (56.25)
Number of metastasis organs	
1	4 (25.00)
2	4 (25.00)
≥3	8 (50.00)
Number of FMT	
1	12 (75.00)
2	2 (12.50)
4	2 (12.50)
Treatment regimen	
Immunotherapy+Chemotherapy+Targeted therapy	4 (25.00)
Immunotherapy+Chemotherapy	6 (37.50)
Immunotherapy+Targeted therapy	3 (18.75)
Chemotherapy/Targeted therapy	3 (18.75)
Combined treatment	
Immunotherapy	13 (81.25)
Radiotherapy	3 (18.75)
Molecular alteration	
EGFR	8 (50.00)
HER-2	1 (6.25)
KRAS	3 (18.75)
TP53	5 (31.25)

Expression of PD-L1	
<1%	4 (25.00)
1%-50%	2 (12.50)
>50%	1 (6.25)
Unknown	9 (56.25)

466

467 **Table 2** Efficacy Evaluation.

468

	Best Efficacy Evaluation		Progression Free Survival	
No.	intracranial	extracranial	intracranial	extracranial
1	PR	SD	6.1	6.8
2	SD	PR	5.8	9.5
3	SD	SD	5.2	3.1
4	SD	SD	6.8	22.5*
5!	SD	PD	4.7	1.0
6!	SD	SD	3.0	3.0
7!	PR	SD	8.4	11.4
8#	PR	SD	6.1	6.1
9#	SD	SD	12.9*	12.9*
10#	PR	PR	12.7*	12.7*
11	PR	SD	10.4	12.2*
12	PR	PR	22.0*	22.0*
13	SD	SD	3.2	6.7
14	SD	PR	7.2	7.2
15	SD	SD	3.8	5.8
16	SD	SD	3.2*	3.2*

	ORR 6/16=37.5%	ORR 4/16=25.0%	Median PFS=6.1m	Median PFS=7.2m
	DCR 16/16=100%	DCR 15/16=93.75%		

*=PFS Not Reached

#=Combined With Cranial Radiotherapy (No.8/10 VMAT, No.9 SRS)

!=Without ICIs

Table 3 Side Effects.

Toxicity	CTCAE 1-2	CTCAE ≥3
Ventosity	5 (31.25)	0
Abdominal colic	3 (18.75)	0
Diarrhea	1 (6.25)	0
Fatigue	4 (25.00)	0
Nausea and vomiting	1 (6.25)	0

Figure Legends

Figure 1 Kaplan-Meier survival curves showing intracranial and extracranial progression-free survival (PFS), as well as overall survival (OS), for the entire cohort. **A** Intracranial PFS of the entire cohort (median PFS, 6.1 months). **B** Extracranial PFS of the entire cohort (median PFS, 7.2 months). **C** OS of the entire cohort (median OS, 13.8 months). The y-axis denotes the percentage of surviving patients, and the x-axis represents follow-up time in months.

Figure 2 Kaplan-Meier PFS curves for patients stratified by EGFR status. **A** PFS curve for

patients with EGFR-resistance (median PFS, 6.8 months). **B** PFS curve for patients with EGFR-negative status (median PFS, 6.1 months). The y-axis denotes the percentage of surviving patients, and the x-axis represents follow-up time in months.

Figure 3 Treatment timeline and phylum-level differential abundance analysis between JSZH_C1 and JSZH_RC1 groups. **A** Schematic diagram of the treatment timeline. **B** Phylum-level differential abundance comparison between JSZH_C1 and JSZH_RC1. JSZH_C1 represents baseline samples; JSZH_RC1 indicates samples obtained after four cycles of FMT combined with six cycles of systemic therapy. Horizontal bar plots show the relative proportion (%) of bacterial phyla for JSZH_C1 (green bars) and JSZH_RC1 (red bars). The middle panel displays inter-group proportion differences with 95% confidence intervals derived from Fisher's exact test. Raw *P*-values and combined effect sizes (ES) for each phylum are listed in the right-hand columns.

Figure 4 Species-level differential abundance analysis between JSZH_C1 and JSZH_RC1 groups. JSZH_C1 corresponds to baseline samples; JSZH_RC1 corresponds to samples collected after four cycles of FMT combined with six cycles of systemic therapy. Horizontal bar plots illustrate the relative proportion (%) of bacterial species in JSZH_C1 (green bars) and JSZH_RC1 (red bars). The middle panel presents proportion differences between the two groups together with 95% confidence intervals calculated by Fisher's exact test. Raw *P*-values and combined effect sizes (ES) for each species are provided in the right-hand columns.

Supplementary Figure 1 Genus-level differential abundance analysis between JSZH_C1 and JSZH_RC1 groups. JSZH_C1 represents baseline samples; JSZH_RC1 represents samples after four cycles of FMT combined with six cycles of systemic therapy. Horizontal bar plots show

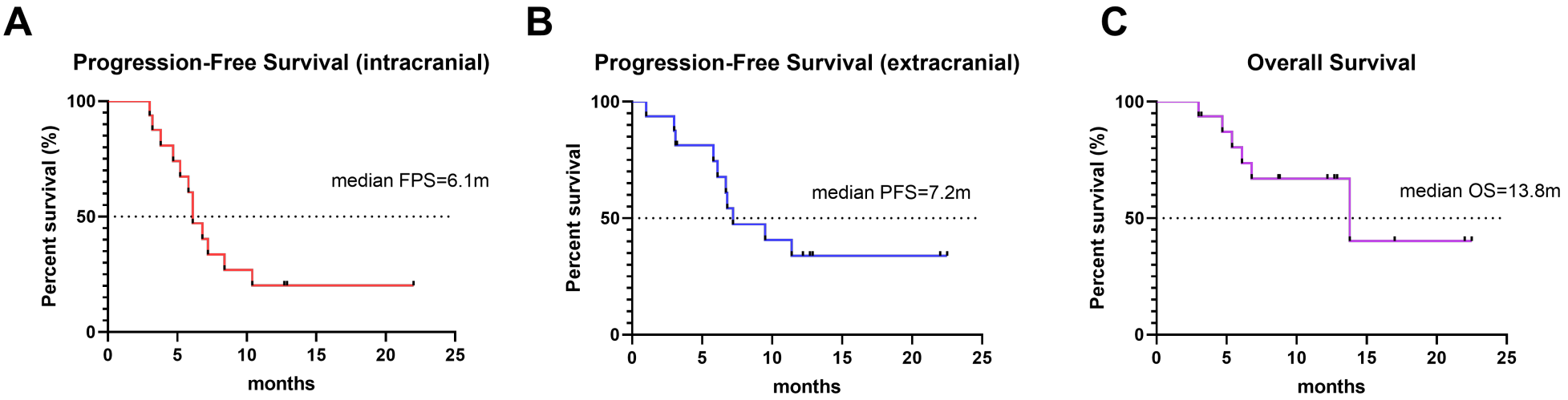
505 the relative proportion (%) of bacterial genera in JSZH_C1 (green bars) and JSZH_RC1 (red
506 bars). The middle panel displays inter-group proportion differences and corresponding 95%
507 confidence intervals based on Fisher's exact test. Raw *P*-values and combined effect sizes (ES)
508 for each genus are listed in the right-hand columns.

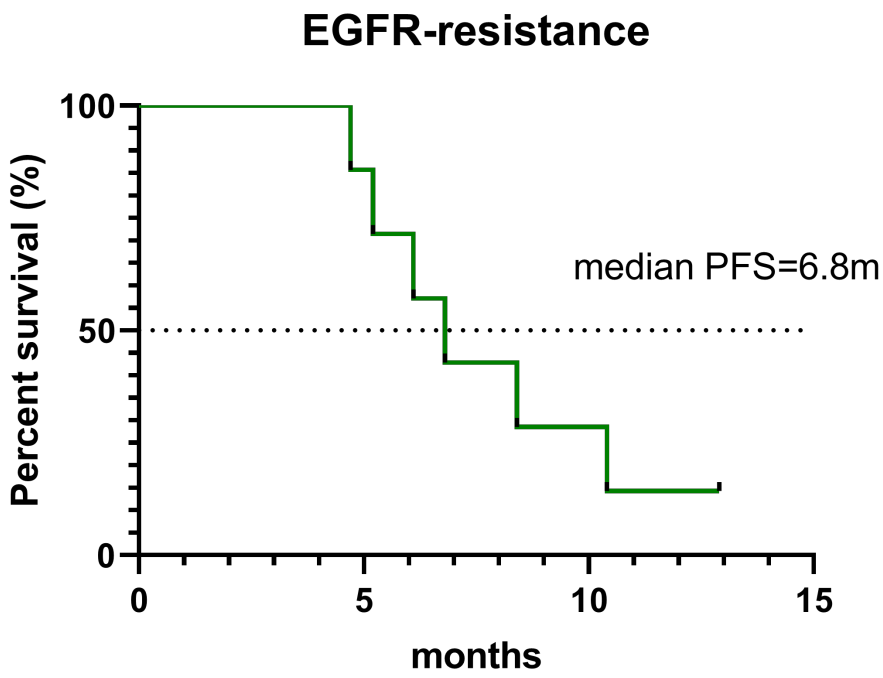
509 **Supplementary Figure 2** Differential abundance of CAZy enzyme families between JSZH_C1
510 and JSZH_RC1 groups. Horizontal bar plots show the proportional distribution (%) of CAZy
511 families for JSZH_C1 (green bars) and JSZH_RC1 (red bars). Fisher's exact test was applied
512 to identify significantly different CAZy families. The middle panel illustrates proportion
513 differences and 95% confidence intervals. *P*-values and combined effect sizes (ES) for each
514 CAZy family are provided on the right.

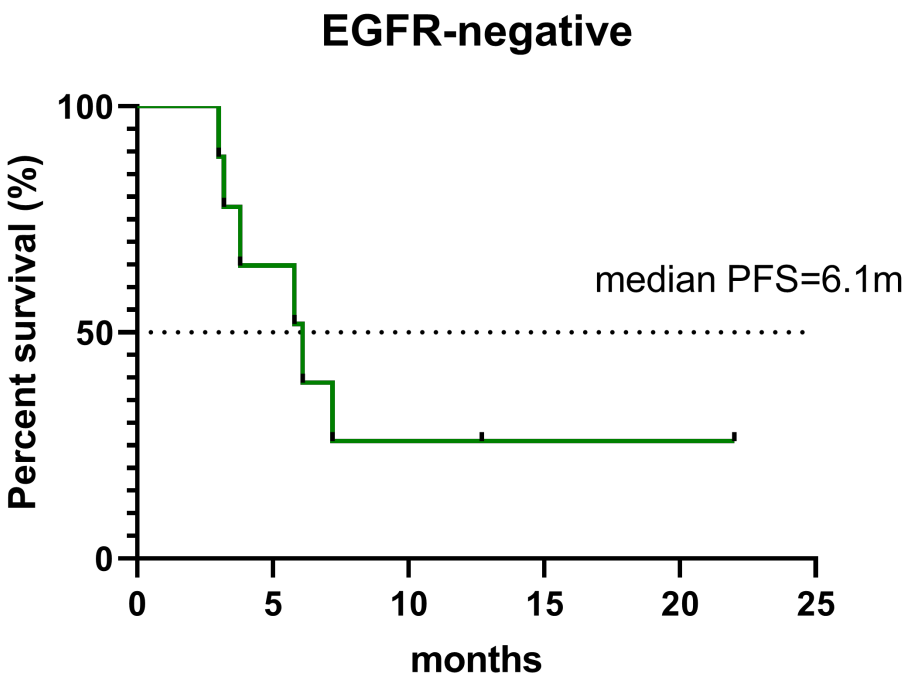
515 **Supplementary Figure 3** Differential abundance of KEGG level-2 functional pathways
516 between JSZH_C1 and JSZH_RC1 groups. Horizontal bar plots represent the proportional
517 distribution (%) of KEGG level-2 pathways in JSZH_C1 (green bars) and JSZH_RC1 (red bars).
518 Fisher's exact test was used to detect inter-group functional differences. The middle panel
519 shows proportion differences and 95% confidence intervals. *P*-values and combined effect
520 sizes (ES) for each KEGG level-2 pathway are listed on the right.

521 **Supplementary Figure 4** Differential abundance of KEGG level-3 metabolic pathways
522 between JSZH_C1 and JSZH_RC1 groups. Horizontal bar plots represent the proportional
523 distribution (%) of KEGG level-3 metabolic pathways in JSZH_C1 (green bars) and JSZH_RC1
524 (red bars). Fisher's exact test was performed to screen significantly different pathways. The
525 middle panel displays proportion differences and 95% confidence intervals. *P*-values and
526 combined effect sizes (ES) for each KEGG level-3 pathway are provided on the right.

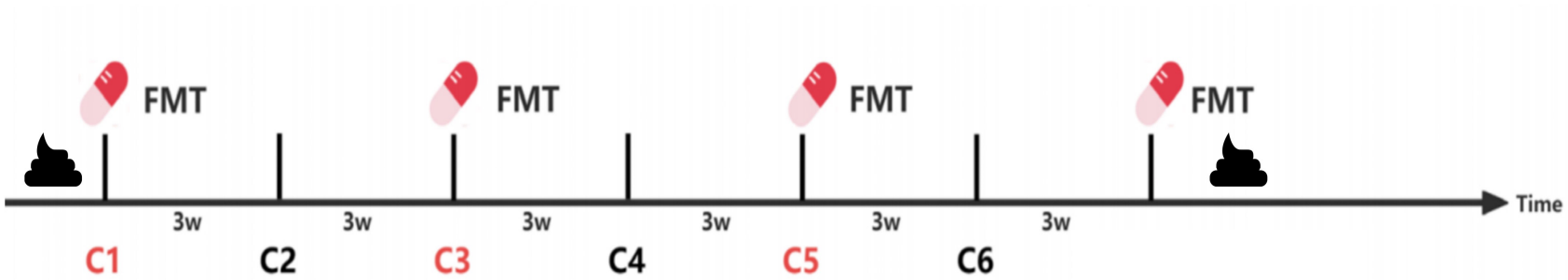
527


A
Progression-Free Survival (intracranial)
Percent survival (%)
100
50
0
0
5
10
15
20
25
months
median FPS=6.1m
B
Progression-Free Survival (extracranial)
Percent survival
100
50
0
0
5
10
15
20
25
months
median PFS=7.2m
C
Overall Survival
Percent survival (%)
100
50
0
0
5
10
15
20
25
months
median OS=13.8m

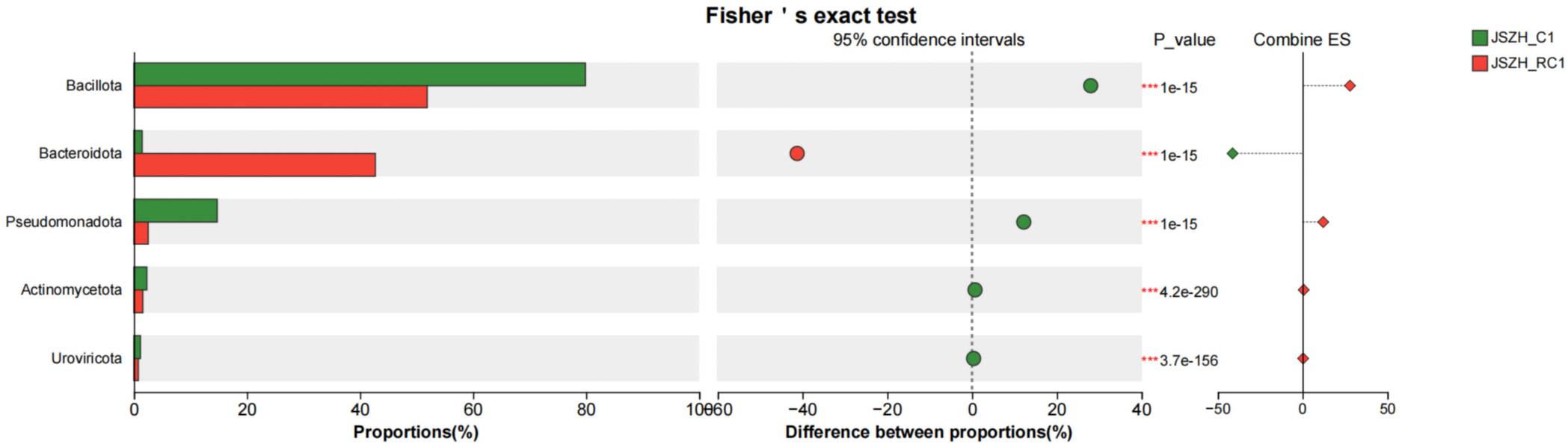

EGFR-resistance
Percent survival (%)
100
50
0
0
5
10
15
months
median PFS=6.8m

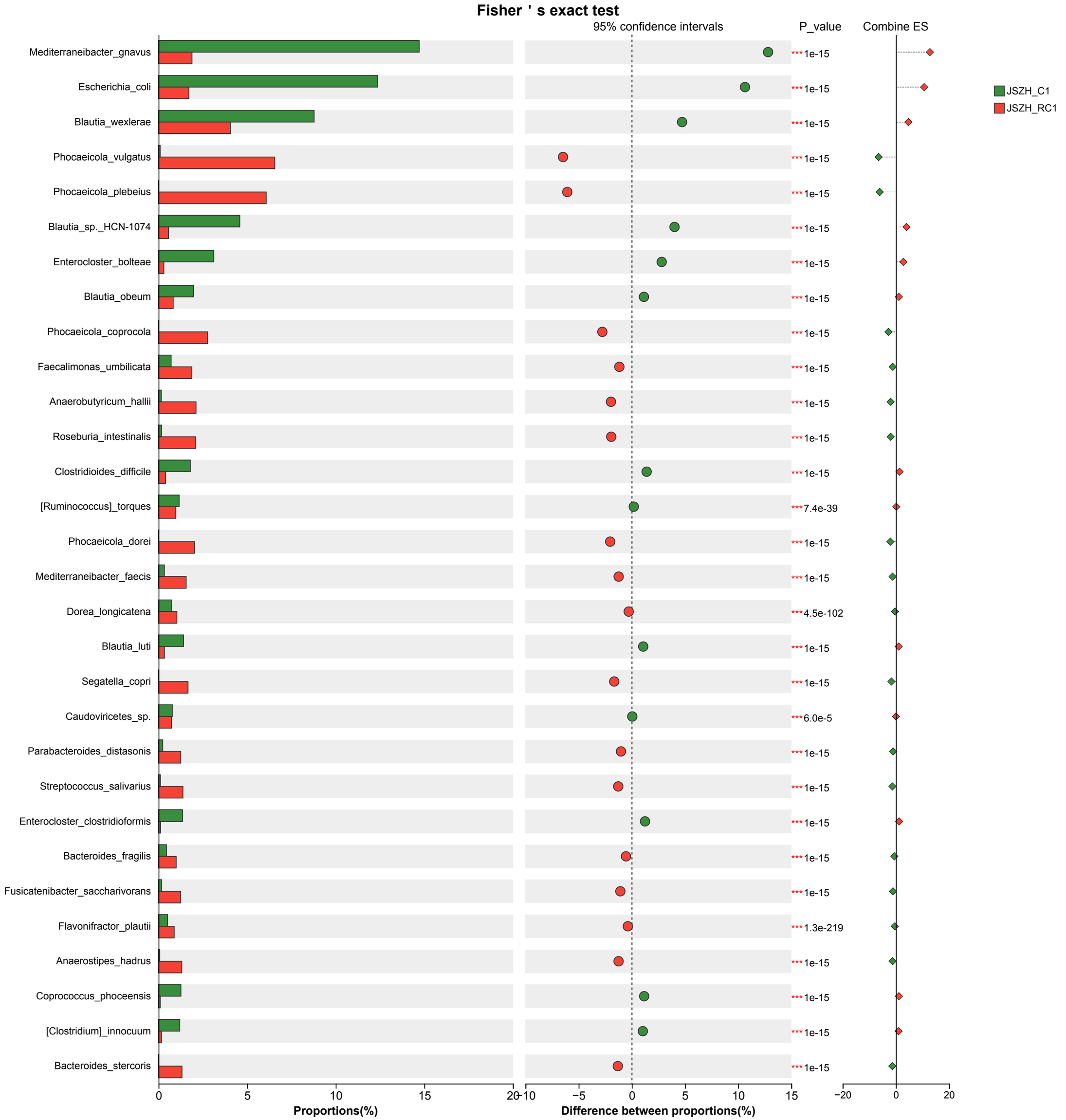

EGFR-negative
Percent survival (%)
100
50
0
0
5
10
15
20
25
months
median PFS=6.1m

A


FMT
FMT
FMT
FMT
Time
3w
3w
3w
3w
3w
3w
C1
C2
C3
C4
C5
C6

B


Fisher ' s exact test
95% confidence intervals
P_value
Combine ES
JSZH_C1
JSZH_RC1
Bacillota
Bacteroidota
Pseudomonadota
Actinomycetota
Uroviricota
***1e-15
***1e-15
***1e-15
***4.2e-290
***3.7e-156
0
20
40
60
80
100
Proportions(%)
60
40
20
0
20
40
Difference between proportions(%)
50
0
50


Fisher ' s exact test
95% confidence intervals
P_value
Combine ES
JSZH_C1
JSZH_RC1
Mediterraneibacter_gnavus
Escherichia_coli
Blautia_wexlerae
Phocaeicola_vulgatus
Phocaeicola_plebeius
Blautia_sp._HCN-1074
Enterocloster_bolteae
Blautia_obeum
Phocaeicola_coprocola
Faecalimonas_umbilicata
Anaerobutyricum_hallii
Roseburia_intestinalis
Clostridioides_difficile
[Ruminococcus]_torques
Phocaeicola_dorei
Mediterraneibacter_faecis
Dorea_longicatena
Blautia_luti
Segatella_copri
Caudoviricetes_sp.
Parabacteroides_distasonis
Streptococcus_salivarius
Enterocloster_clostridioformis
Bacteroides_fragilis
Fusicatenibacter_saccharivorans
Flavonifractor_plautii
Anaerostipes_hadrus
Coprococcus_phoceensis
[Clostridium]_innocuum
Bacteroides_stercoris
***1e-15
***7.4e-39
***4.5e-102
***6.0e-5
***1.3e-219
0
5
10
15
20
−10
−5
0
5
10
15
−20
0
20
Proportions(%)
Difference between proportions(%)

Supplementary Files

This is a list of supplementary files associated with this preprint. Click to download.

- Coverletter.docx
- SupplementaryFigure1.pdf
- SupplementaryFigure2.pdf
- SupplementaryFigure3.pdf
- SupplementaryFigure4.pdf